European Journal of Engineering and Technology Research
Vol 9 | Issue 1 | February 2024
ISSN 2736-576X

CrossMark

RESEARCH ARTICLE

Experimental Investigation of Void Coalescence in XTral-728 Plate Containing Three-Void Cluster

Mohammad Atiqur Rahman[1], Md Mesbah uddin[2,*], and Latiful Kabir[3]

ABSTRACT

Void clustering effect is investigated by performing uniaxial tensile test on commercial 95% aluminum alloy XTral 728 by strategically placing an additional hole. Incorporating additional void induces strong stress and strain localization and reduces incipient coalescence strain approximately 17%. Also, two different cluster orientations with respect to applied loading and hole spacing ratios have been considered. The experimental revealed that material ductility is significantly decreased with increasing hole spacing ratios and for certain cluster orientation. To evaluate existing void coalescence models, numerical simulations are also performed and found that existing models overestimate the incipient coalescence strains for considered three-void cluster.

Keywords: Cluster, ductile fracture, material science, void coalescence.

Submitted: October 09, 2023

Published: February 16, 2024

10.24018/ejeng.2024.9.1.3116

[1] *Mechanical Integrity & Reliability Engineer, Zeon Chemicals L.P, USA.*
[2] *Data Scientist, Wallace Distribution, USA.*
[3] *Mechanical Engineer, USA.*

****Corresponding Author:***
e-mail: mesbahuddin1991@gmail.com

1. Introduction

Void clusters are closely spaced voids nucleated form cluster of inclusion in structural metals. Presence of clusters in structural metals enhance void interaction and thereby void growth and coalescence [1]. Magnusen *et al.* [2] examined a tensile specimen containing random and regular arrays of holes and found that the specimen containing random arrays are less ductile than regular arrays [2]. Bandstra and Koss [3] showed numerically that strain localization behavior within microstructure that contains void cluster is remarkably higher than those containing uniformly spaced voids [3]. Dubinsky and Koss [4] examined experimentally the dependence of ductile fracture on the size and distribution of voids. They physically modeled random and regular arrays of equal sized holes within tensile specimen of 1100-0 Al sheet and 7075 Al plate and sheet and observed that increasing hole spacing, which decrease the degree of hole clustering, increases both strength and ductility and conversely, decreasing the hole size causes a minor increase in both strength and ductility [4]. Thomson *et al.* [5] considered three linear clustered particles embedded in a three-dimensional unit cell under triaxial loading conditions and observed that orientation of cluster with respect to the major loading direction has significant influence on failure strain [5]. Zhang and Chen [6] considered the effect of stress state on void coalescence by employing unit cell containing a void cluster and proposed a coalescence criterion in which critical void volume fraction is expressed in terms of stress triaxiality [6].

These studies addressed void coalescence behaviour within linear cluster; they did not consider non-linear cluster which is asymmetric to the surrounding material. Geltmacher *et al.* [7] observed that three-void cluster accelerates void growth and coalescence in certain microstructures [7]. Colapietro *et al.* [8] also monitored that fracture surface of Cu containing equiaxed particles shows many equiaxed dimples with three-fold symmetry. They developed a specimen containing three blind-end holes with hemispherical ends to model three-void cluster and found characteristic three-fold symmetry upon specimen fracture. They suggested that three-void clusters-oriented transverse to tensile axis accelerate void growth and coalescence; therefore, three-void cluster is a special case of interest [8]. Based on the experimental result of Colpietro *et al.* [8], Bandstra and Koss [9] performed a finite element simulation of the experiment and observed that the void growth rate within the cluster is sensitive to strain hardening and noticed that a load limit develops within the inter-void ligament [9]. Later, Bandstra and Koss [10] performed a three-dimensional finite element analysis of RVE containing a cluster of three closely spaced voids within a plane normal to deformation axis to examine the sensitivity of void growth and coalescence to strain hardening, stress state and inter-void spacing. They showed that coalescence is accelerated by increasing stress

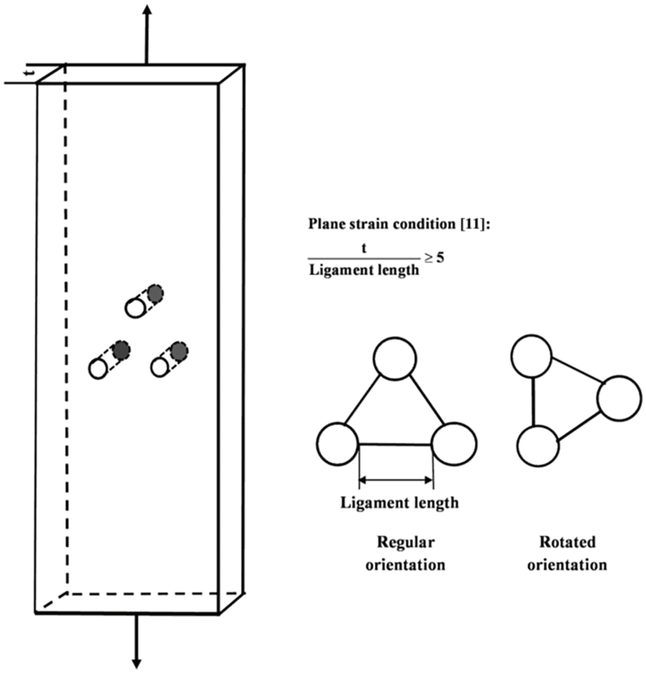

Fig. 1. Schematic of the specimen geometry used for the experiments. Note: Two different orientations of void cluster with respect to the loading direction.

triaxiality and decreasing strain hardening and inter-void spacing within cluster [10].

In the present work, three-void clusters are studied. Two different spacing ratios and two different orientations with respect to principal loading direction are considered. Finite element simulations of the experiment were performed. The use of the digital image correlation technique in the experiments enabled tracking of the local deformation in the ligament. The experimental and numerical results are compared and found to be in good agreement. The numerical results have been used as a framework to evaluate existing void coalescence models.

2. Experimental Method

The tensile testing experiments were performed using 100 mm long and 30 mm wide, and 7 mm thick XTral 728 metal plate containing void clusters. These macroscopic holes are assumed to behave like micro-voids within the real microstructure during void coalescence. Two inter-hole spacing ratio ($\chi_o = 0.4$ to 0.5) and two cluster orientations (referred to as "regular orientation" and "rotated orientation" in Fig. 1) are considered in the present work.

The plane strain condition between manufactured holes is necessary for appropriate void coalescence modelling. Thomason [11] stated that the constraint factor for plane stress plastic deformation between two holes is much lower than those encountered for similar plane strain and three-dimensional conditions. He analytically showed that for the plane stress condition, plastic deformation localises between the holes immediately after the first small increment of plastic deformation, and only small levels of void growth would be required to initiate void coalescence. Therefore, the plane stress condition is not suitable for modelling void coalescence, and the plane strain condition is enforced in the present work by specifying the required condition on the specimen design.

The specimens were made 100 mm long and 30 mm wide. The length was chosen so that there would remain enough gripping area when mounted in Instron machine and the applied load could be assumed as far-field with respect to the void cluster. The width of the specimen was selected 30 mm to ensure minimum edge effects (no interaction between void cluster and specimen edge was observed). Also, the hole diameter was selected by keeping the spacing ratios constant (0.4 and 0.5) between the voids for two different cluster orientation. The hole diameter was calculated for two spacing ratio values, $\chi 0 = 0.4$ and 0.5 and constant thickness/ligament length = 5 (specimen thickness 7 mm and ligament length 1.4 mm) to maintain Thomason's [11] plane strain condition. The ligament length was kept constant (1.4 mm) throughout the experiment to ensure that the thickness/ligament-length ratio effect would not have any impact on coalescence strain. Griffin [12] numerically showed that to model void coalescence under plane strain condition, it is necessary to keep the ratio of specimen thickness to ligament length constant; the coalescence strain would be altered for different ratios of thickness to ligament-length value when on the domain thickness/ligament-length <10. Larger values of thickness/ligament length could be selected, but this would essentially decrease ligament length below 1 mm when using 7 mm thick plate. Griffin's [12] results suggested that the utilized DIC system is incapable of capturing local strain when the ligament length falls below 1 mm. The drill-bits sizes were chosen close to the calculated hole diameters, giving slightly different void spacing ratios than the nominal values. Table I shows the nominal and actual spacing ratio values. For convenience, the nominal spacing ratio values will be referred to throughout the document.

After manufacturing, the specimens were cleaned with soap and water to remove dirt and particles from the machined surface. Then the samples were cleaned with alcohol to encourage paint adhesion, because the relative movement between the paint layer and the metal surface would result in erroneous strain measurement. White primer was applied to coat the surface and then a high-density black speckle paint layer was applied to facilitate use of the DIC system. A high-density speckle pattern was created on every specimen. In addition, the far-field principal strains obtained from the extensometer were in excellent agreement with the DIC far-field principal strain values. These results suggest that the DIC system is a reliable strain measurement technique and local strain extracted from the DIC could safely be used to quantify deformation in the inter-void ligament. The local strain obtained from the DIC method was used to calculate the ligament flow stress using the Voce equation.

Aluminum alloy (XTral 728) was used to prepare samples containing three-void clusters. XTral 728 has excellent formability, improved resistance to corrosion and high surface quality. Its light weight makes it attractive to the industrial vehicle bodywork; specially to build tankers to transport dangerous materials.

TABLE I: The Nominal and Actual Spacing Rations Values of the Specimen

χ_0	Calculated radius (mm)	Calculated diameter (mm)	Actual drilled diameter (mm)	Actual χ_0	Ligament length (mm)	Drill bit description
0.4	0.4666	0.933	0.9398	0.401658261	1.4	#63, 0.9398 mm
0.5	0.7	1.400	1.397	0.499463711	1.4	#54, 1.397 mm

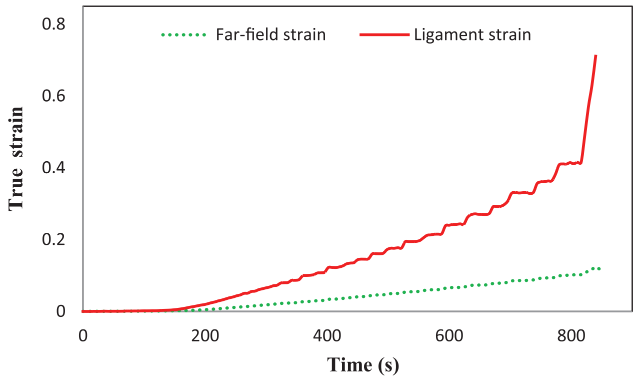

Fig. 2. Strain history showing localization of strain in the inter-hole ligament compared to far-field strain for rotated cluster with hole spacing ratio, $\chi_0 = 0.5$.

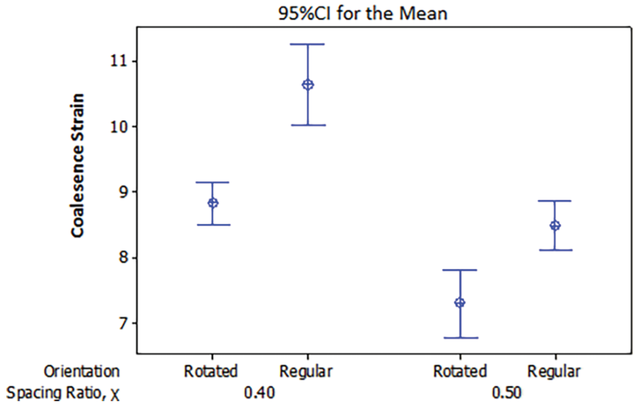

Fig. 3. Experimental IC strain for each geometry with 95% confidence interval for the mean.

The true stress–true strain curve in the rolling direction obtained from a dog bone specimen uniaxial test was fitted with the Voce [13] hardening law. The material flow rule expressed by the Voce equation is:

$$\overline{\sigma} = \sigma_s - \left(\sigma_s - \sigma_y\right) \exp\left[-\alpha \left(\varepsilon^p\right)^\beta\right] \quad (1)$$

where $\overline{\sigma}$ is the flow stress, σ_s is the ultimate tensile stress and σ_y is the yield stress and ε^p is the plastic strain, and $\alpha$and β are fitting parameters. The values of these parameters were found by fitting the experimental data with the Voce hardening rule. The Voce equation for XTral 728 is:

$$\overline{\sigma} = 394.11 - (394.11 - 146) \exp\left[-14.1 \left(\varepsilon^p\right)^{1.09}\right] \quad (2)$$

3. Results and Discussions

3.1. *Effect of Void Clustering*

Due to local deformation, the ligament experienced severe strain compared to the whole specimen which can be noticed from the DIC results showing far-field principal strain beside the ligament strain history in Fig. 2 Similar strain localization behaviour was noticed from the numerical results.

3.2. *Experimental IC Strains*

The experimental results of far-field principal strains obtained from DIC and extensometer at the incipient of coalescence and ligament fracture are presented in tabular form. The principal strains at incipient coalescence and ligament fracture for each sample is averaged and standard deviations are also computed. Fig. 3 shows the experimental DIC results for IC strains with 95% confidence interval. The IC strains decreases 19.68% for regular cluster orientation while it is 17.4% for rotated orientation when the inter-hole spacing ratio increase from $\chi_o = 0.4$ to 0.5. On the other hand, the rotated cluster shows 17.61% decrease in IC strain for spacing ratio $\chi_o = 0.4$ and 15.25% for spacing ratio $\chi_o = 0.5$ when compared to regular orientation. These results are in good agreement with numerical results and prediction from various PLL model.

The experimental microstructure variables are compared to numerical results at incipient coalescence, and excellent agreement is found. The microstructure variables that are compared are horizontal and vertical hole diameter, hole aspect ratio, ligament length, void spacing ratio and far-field load. These parameters are also important for PLL calculation. The comparison is presented in a tabular form in Table II, and a per cent difference is also provided when compared to numerical results.

Within the rotated cluster, the hole in the middle simultaneously interacts with the other two holes in the angled positions and experiences larger growth than the other two holes, as shown in Fig. 4. Therefore, localization occurs promptly in the rotated cluster, and lower IC strains are observed when compared to the regular cluster orientation. The middle hole dimension is measured here for calculating void aspect ratio and spacing ratio for rotated cluster. For the regular cluster, the ligament perpendicular to the principal load fractures; therefore, those holes dimensions are measured using *Image Pro Plus* software for calculating void aspect ratio and spacing ratio. Also, qualitatively the image corresponding to IC is compared to FE mesh and similarity in void shape evolutions is noticed as showed in Fig. 5. The figures show qualitative agreement of the hole contours at the instant of IC.

4. Evaluation of Present Coalescence Models

The available plastic limit load (PLL) models predict coalescence strain based on load limit of the inter-void ligament for matrix containing a periodic array of voids. These models account for stress state, void shape, spacing and strain hardening exponent. However, these PLL models do not explicitly consider the matrix where closely spaced

TABLE II: Effect of Spacing Ratio and Orientation on IC Strain

	Spacing ratio effect $\chi_o = 0.4 \rightarrow 0.5$		Orientation effect Regular $\rightarrow$ Rotated	
	Regular	*Rotated*	$\chi_o = 0.4$	$\chi_o = 0.5$
Decrease (%)	19.68%	17.40%	17.61%	15.25%

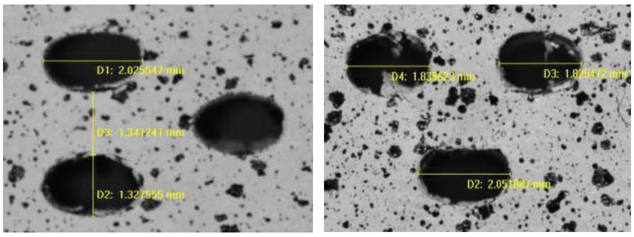

(a) (b)

Fig. 4. Measurement of important void dimension using *Image Pro Plus* at the incipient of coalescence for: (a) regular cluster and (b) rotated cluster with spacing ratio, $\chi_o = 0.5$.

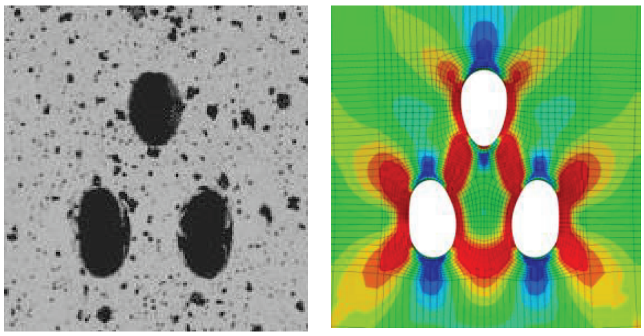

(a) Regular cluster orientation with χ_O=0.5.

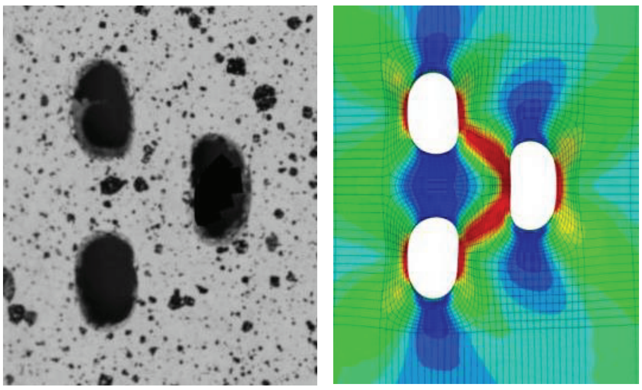

(b) Rotated cluster orientation with χ_O=0.5.

Fig. 5. Comparison of experimental image and FE deformed mesh at the instant of IC for: (a) regular cluster and (b) rotated cluster with $\chi_o = 0.5$.

voids are not periodically distributed and not oriented orthogonally with the loading direction such as the three-void clusters used in the present work. The experimental and numerical results obtained in the work are employed in this section to assess existing PLL models.

4.1. *Thomason's Cylindrical Model*

Thomason's [11] PLL model, as described by (3) for cylindrical holes, provides the best match with the current experimental results of IC strains for the considered three-void clusters, as shown in Fig. 6.

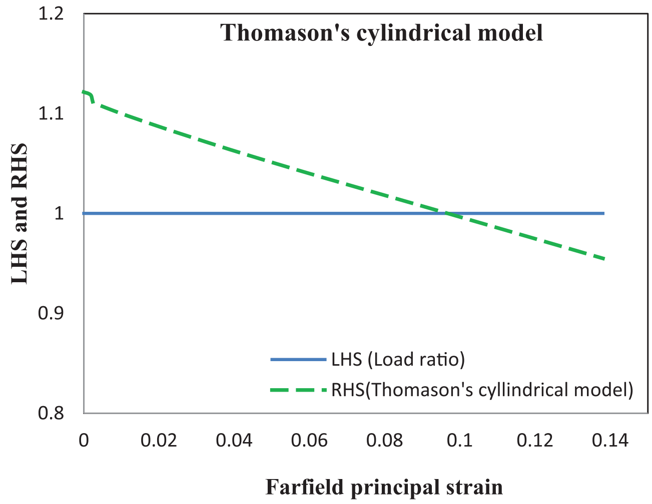

Fig. 6. Prediction of IC strain from Thomason's cylindrical PLL model for regular cluster orientation with spacing ratio, $\chi_o = 0.5$.

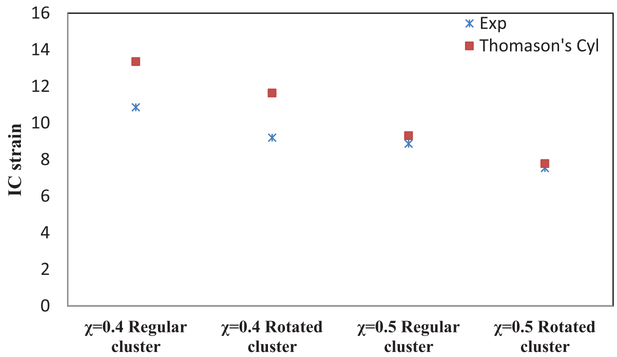

Fig. 7. Comparison of experimental IC strains with Thomason's cylindrical PLL model.

$$\left\{\frac{0.3\,(1-\chi)}{W\chi} + 0.6\right\}\left(1 - \frac{\pi}{4}\chi_o^2\right) = \frac{1}{2} + \frac{\sigma_m}{Y} \tag{3}$$

Thomason's model does not consider the influence of void clustering (interaction of more than two voids) and therefore his model over predicts the IC strains. In addition, for a rotated cluster, localization occurs simultaneously in two angled ligaments which significantly lowers IC strain; his model does not account for the coalescence of voids that are separated by a ligament which is not normal to the far-field principal loading. However, Thomason's model provides close agreement with experimental results for spacing ratio, $\chi_o = 0.5$, but over-predicts for spacing ratio, $\chi_o = 0.4$ for both types of cluster orientation as shown in the Fig. 7.

4.2. *Modified Ragab's Model*

To calculate plastic limit load (PLL) within cluster, Griffin [12] adapted Ragab's (2004) model by incorporating the

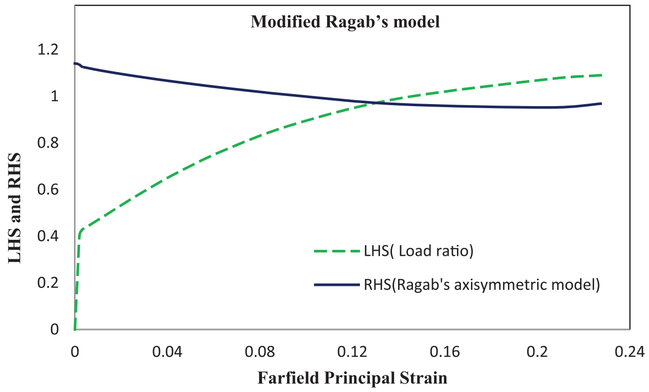

Fig. 8. Estimation of the IC strain from modified Ragab's model for rotated cluster orientation with spacing ratio, $\chi_o = 0.4$.

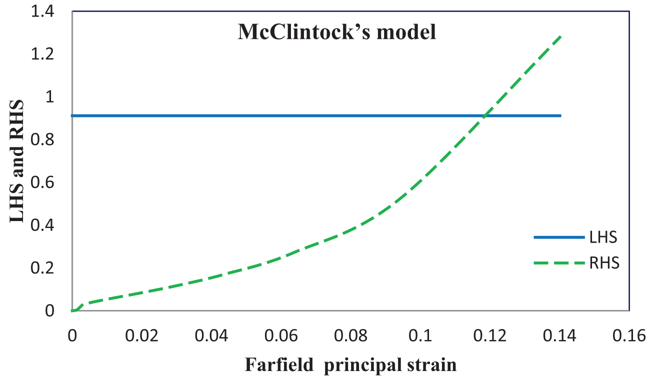

Fig. 10. Prediction of ligament failure strain from McClintock's model [14] for rotated cluster with spacing ratio, $\chi_o = 0.4$.

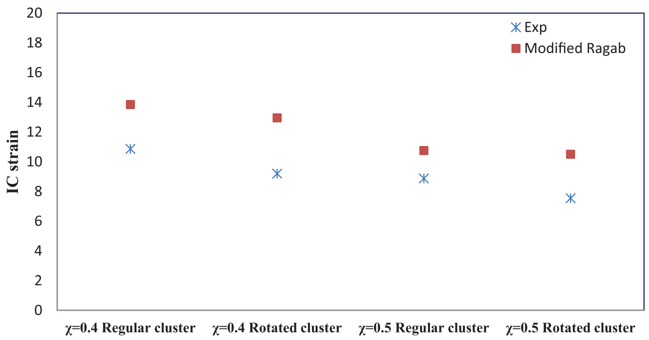

Fig. 9. Comparison of experimental IC strains with prediction from Modified Ragab's model.

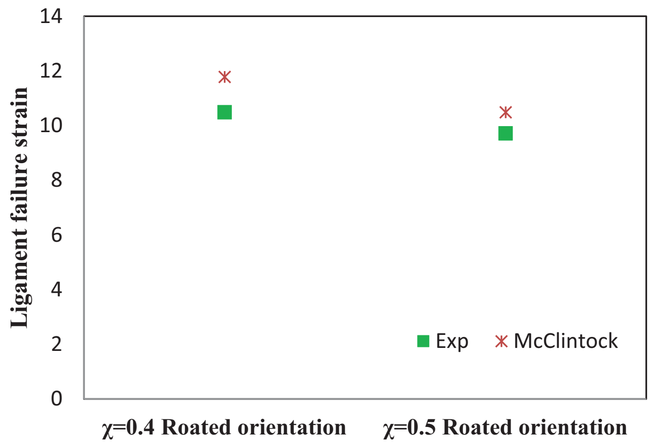

Fig. 11. Comparison of experimental ligament failure strain with McClintock's model [14] for rotated cluster orientation with spacing ratios, $\chi_o = 0.4$ and 0.5.

ligament flow stress, as per (4):

$$\frac{\sigma_1}{\sigma_{UTS}} = \left(1 + \frac{2W^2}{\frac{1}{\chi} - 1}\right) \log\left[1 + \frac{1}{2W^2}\left(\frac{1}{\chi} - 1\right)\right] \left(1 - (\pi/4)\,\chi^2\right) \tag{4}$$

It is observed that ligament flow stress completely saturates at incipient coalescence, which justified the use of modified form of Ragab's model as shown in Fig. 8. The modified Ragab's model over predicts IC strain for each cluster geometry and this trend is higher for rotated cluster orientations as shown in Fig. 9. As observed from the experimental and numerical results, the limit load attained at lower principal strain for a rotated cluster arrangement when compared to a regular cluster. The modified Ragab's model estimates almost similar strain for both cluster orientations, while the experimental results show that the rotated orientation is more prone to coalescence.

4.3. *McClintock's Model*

McClintock's model [14], described by (5), accurately predicts the ligament fracture strain for the rotated cluster, as illustrated in Fig. 10.

$$\ln\left(\frac{1}{\chi}\right) = \ln\sqrt{1+\gamma^2} + \frac{\gamma}{2\,(1-N)} \sinh\left(\frac{(1-N)\,\sigma}{\tau}\right) \tag{5}$$

As shown in Fig. 11, the fracture of the ligament takes place between the angled ligaments for the rotated cluster. McClintock's model accounts for shear and thereby is able to predict the fracture strain of rotated clusters. This is also in agreement with unit cell investigation under simple shear by Rahman *et al*. [15]. McClintock's model does not consider failure of the ligament normal to load and fracture occurs at the ligament normal to the load for regular cluster and cannot be predicted by McClintock's model. Similar to Thomason's cylindrical model, McClintock's model is also developed for cylindrical holes under a plane strain assumption, which is similar to the present work.

5. Conclusion

An experimental and numerical study of a three-void cluster under uniaxial loading was carried out, and the results were compared. The obtained results show that cluster orientation with respect to loading direction significantly altered material ductility and reduced IC strain by approximately 17% for the rotated three-void cluster when compared to the regular cluster. In addition, increasing spacing ratio of the holes within a cluster also reduced IC strain significantly. The experimental and numerical results show excellent agreement for the important microstructural parameters such as void aspect ratio, spacing ratio and load at the incipient coalescence. However, the existing void coalescence models overestimate IC strain, which suggests the development of an advanced damage model to describe incipient coalescence for clusters. The results obtained in this work could be employed to development of PLL model accounting cluster effect.

5.1. *Future Research*

Recently computational modelling and machine learning has been used for different application including void cluster, material science and so on [15]–[22]. In future we would like to further study leveraging modern computational tools which will allow us to study with different combinations of experimental parameters.

Acknowledgment

The authors gratefully acknowledge the Natural Science and Engineering Research Council of Canada (NSERC) and Auto 21 Network of Centers of Excellence for providing financial support to this work.

Conflict of Interest

Authors declare that they do not have any conflict of interest.

References

[1] Bandstra J, Koss DA. On the influence of void clusters on void growth and coalescence during ductile fracture. *Acta Materialia*. 2008;56. doi: 10.1016/j.actamat.2008.05.009.

[2] Magnusen PE, Dubensky EM, Koss DA. The effect of void arrays on void linking during ductile fracture. *Acta Metallurgica*. 1988;36:1503–9. doi: 10.1016/0001-6160(88)90217-9.

[3] Bandstra JP, Koss DA. Modeling void coalescence during ductile fracture of a steel. *Mater Sci Eng A*. 2004;366(1):269–81.

[4] Dubinsky J, Koss DA. Void interaction effects on ductile fracture. *Acta Metall*. 1987;35(10):2431–42.

[5] Thomson RC, Hancock JW, Lindgren LE. Micromechanics of failure in three dimensions. *Eng Fract Mech*. 2003;70(3–4):413–24.

[6] Zhang K-S, Chen X-M. Effect of stress state on void coalescence. *Acta Mater*. 2009;57(9):2692–701.

[7] Geltmacher AB, Matic P, Zok FW. Image-based modeling of the response of experimental three-void clusters in ductile metals. *Acta Mater*. 1996;44(8):3205–20.

[8] Colapietro D, Dodds RH Jr, Needleman A. Void growth and coalescence in round bars with particles. *Int J Fract*. 2001;109(2):169–90.

[9] Bandstra JP, Koss DA. Modeling side void growth and coalescence in crystals containing two in-line voids. *Acta Mater*. 2004;52(2):345–56.

[10] Bandstra JP, Koss DA. Simulation of void growth from clustered particles in three dimensions. *Mater Sci Eng A*. 2008;497(1–2): 39–51.

[11] Thomason PF. *Ductile Fracture of Metals*. 1st ed. Oxford: Pergamon Press; 1990.

[12] Griffin TB. The influence of microstructural morphology on ductile fracture by void growth and coalescence [dissertation]. Gainesville (FL): University of Florida. 2012.

[13] Voce E. The relationship between stress and strain for homogeneous deformation. *J Inst Met*. 1948;74:537–62.

[14] McClintock FA, Kaplan SM, Berg CA. Ductile fracture by hole growth in shear bands. *Int J Fract*. 1966;2:614–27.

[15] Williamson DJ, Burn GL, Simoncelli S, Griffie J, Peters R, Davis DM, *et al.* Machine learning for cluster analysis of localization microscopy data. *Nat Commun*. 2020;11:1493. doi: 10.1038/s41467-020-15293-x.

[16] Ahamed S, Uddin MM. Addressing computational challenges in physical system simulations with machine learning [Internet]. arXiv preprint arXiv:2305.09627v1, 2023 May 10 [cited 2023 Jan 3]. doi: 10.48550/arXiv.2305.09627.

[17] Ahamed S, Uddin MM. Estimating uncertainty of earthquake rupture using bayesian neural network [Internet]. ArXiv:1911.09660 [physics, stat], 2019 Nov [cited 2023 Jan 3]. Available from: https://arxiv.org/abs/1911.09660v2.

[18] Uddin MM. Studying the scratching behavior of Nb/NbcNanolaminate using molecular dynamics atomistic simulations. Northern Illinois University ProQuest dissertations publishing. 2020. pp. 27999015.

[19] Uddin MM. Finite difference analysis of stress distribution around an elliptical hole in a plate subjected to axial loading. *Int J Mod Dev Eng Sci*. 2023;2(4):1–4. Available from: https://journal.ijmdes.com/ijmdes/article/view/119.

[20] Uddin MM. Study the effect of scratching depth and ceramic-metal ratio on the scratch behavior of NbC/Nb Ceramic/Metal nano-laminates using molecular dynamics simulation and machine learning [Internet]. arXiv preprint arXiv:2305.03698v1, 2019 May 14 [cited 2023 Jan 3]. doi: 10.48550/arXiv.2305.03698.

[21] Uddin MM, Akhtaruzzaman R, Shanto TA, Hasan MN. Study the performance of a dynamic wall heat exchanger using computational fluid dynamics. *Eur J Eng Technol Res*. 2023;8(3):2023. doi: 10.24018/ejeng.2023.8.3.3043.

[22] Uddin MM. Study the effect of different ellipse sizes on the stress distribution around an elliptical hole in a plate subjected to axial loading using finite difference analysis. *IOSR J Mech Civil Eng (IOSR-JMCE)*. 2023;20(2III):37–41. doi: 10.9790/1684-2002034257.